

Mechanical and acid-etching properties of $\text{Bi}_2\text{O}_3\text{--ZnO--B}_2\text{O}_3$ glass-containing ceramic fillers

Woogyung Sung · Jinho Kim · Seongjin Hwang ·
Hyungsun Kim

Received: 13 July 2007 / Accepted: 18 December 2007 / Published online: 3 April 2008
© Springer Science+Business Media, LLC 2008

Abstract The properties of the composite, having a complicated microstructure, are decided by many factors such as those of glass matrix, crystal phases, fillers, and holes. We investigated how the addition of ceramic fillers to the glass matrix affects the mechanical and etching properties of the glass composite by forming new crystal phases. Different amounts of two fillers, ZnO and Al_2O_3 , were added to a glass frit consisting of $\text{Bi}_2\text{O}_3\text{--ZnO--B}_2\text{O}_3$. It was sintered at 550 °C for 30 min. Based on the results of this study, the porosity and degree of crystallization of the composites could be controlled by adjusting the content of the ZnO and Al_2O_3 fillers. Therefore, porosity and degree of crystallization formed by the reaction between a glass matrix and fillers influence the mechanical and etching properties of the composite.

Introduction

Plasma display panels (PDPs) are self-emitting display devices that produce light through the discharge of a gas. Barrier-ribs located on the rear substrate play an important role in forming the space required for discharge and preventing cross-talk from the adjacent sub-pixels in the PDP. Microelectronic devices have seen a dramatic amount of development in recent years, such that today's devices offer high performance, small size, high quality, and low cost, and are produced by a simple process [1–3]. For the same reason, the barrier-rib forming methods have been

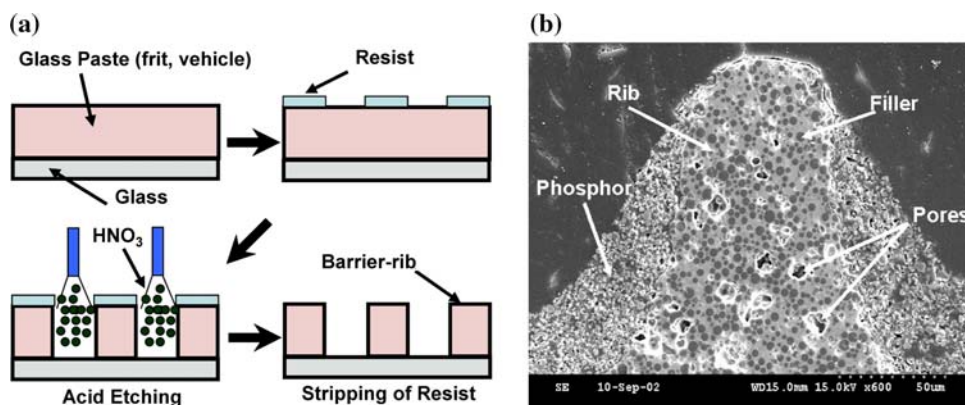
changed. Various barrier-rib forming methods were initially proposed, including screen printing, sandblasting, acid etching, injection molding, lift-off, rolling of green tape, photolithographic process, and the UV-LIGA process [3]. The screen-printing and sandblasting methods have been used since the early period of the PDP industry. However, these processes are not suitable for high-definition displays, due to the complexity of the process and difficulty in achieving minute patterning. Among these various methods, acid etching is currently used in the PDP industry (Fig. 1).

From the viewpoint of the materials used for barrier-ribs, there are some technical issues which remain to be resolved in the display industry, due to the RoHS (Restriction of Hazardous Substances) and WEEE (Waste Electrical and Electronic Equipment) specifications [4]. Therefore, many studies on barrier-ribs are in progress to replace the lead glasses with lead-free glasses [5–8]. Since bismate and lead glasses have similar atomic weights and physical properties, the bismate-based glass system has been widely used and developed as an eco-material to replace lead-based glass for various components in PDPs, such as barrier-ribs, and dielectric and sealing materials [4, 9].

When replacing lead-based glasses with lead-free glasses, it is necessary to investigate the effect of adding ceramic fillers to the lead-free glass matrix. Al_2O_3 and ZnO ceramic fillers, which were commercially used in the lead-based glass system, play important roles from several viewpoints. The role of Al_2O_3 filler is mainly to reinforce the mechanical properties that can prevent the destruction on handling during process (passage and use). According to several reports, the effect of ZnO, Al_2O_3 , MgO, and TiO_2 ceramic fillers on thermal, optical, electrical, and mechanical properties has been reported [8, 10–12]. However, the roles of ceramic fillers on etching property

W. Sung · J. Kim · S. Hwang · H. Kim (✉)
School of Materials Engineering, Inha University,
253 Younghyun-dong, Nam-gu, Incheon 402-751, Korea
e-mail: kimhs@inha.ac.kr

Fig. 1 (a) Schematic diagrams of acid-etching process for barrier-ribs in plasma display panel and (b) cross-section micrograph of barrier-ribs showing a complex microstructure composed of pores and fillers in a glass matrix



have not been clear in lead-free glass system. After acid-etching process for barrier-ribs, the sidewall of the barrier-rib should have a rough surface indicating that the phosphors (Red, Green, Blue) can be physically bonded onto the barrier-ribs in the subsequent process (Fig. 1b).

In this study, we investigated lead-free-based glass, bismate glass, with the ratio of mixing fillers on mechanical and etching properties. The purpose of our study is to determine the effect of adding ceramic fillers on the mechanical and etching properties of barrier-ribs with a bismate glass matrix.

Experimental procedures

For the fabrication of the $12\text{Bi}_2\text{O}_3\text{--}55\text{ZnO--}32\text{B}_2\text{O}_3\text{--}1\text{Al}_2\text{O}_3$ glass (in mol%), the glass composition was prepared from chemically pure reagents, Bi_2O_3 (99.9%, Aldrich Chemical Co., USA), ZnO (99.9%, Aldrich Chemical Co., USA), H_3BO_3 (99.99%, Aldrich Chemical Co., USA), and Al_2O_3 (99%, Aldrich Chemical Co., USA). The batch was well mixed by ball milling for 12 h and then melted in an alumina crucible at $1,200\text{ }^\circ\text{C}$ for 1 h. The melt was quenched into a stainless roller to make glass cullets. The quenched glass was pulverized to an average particle size of $2.5\text{ }\mu\text{m}$ using a planetary mono mill with zirconia balls and a container for 5 h. The two fillers, ZnO ($d_{50} = 0.5\text{ }\mu\text{m}$) and Al_2O_3 ($d_{50} = 2.5\text{ }\mu\text{m}$), were added to the glass matrix in various amounts. The glass frit and ceramic fillers were well mixed by ball milling for 12 h and dried at $130\text{ }^\circ\text{C}$ for 24 h. The compositions of the two fillers-added specimens are shown in Table 1. The mixture powder was then uniaxially pressed into a disk shape at about 1.3 kgf/cm^2 , followed by densification at $550\text{ }^\circ\text{C}$ for 30 min in air.

The glass transition temperature and crystallization peak of the glass matrix and the glass composites with ceramic fillers were determined using a differential thermal analyzer (DTA, Thermo Plus TG-8120, Rigaku, Japan). The porosity and density of the samples were measured

Table 1 Batch of composition (in wt.%), the glass frit, and ceramic fillers (ZnO , Al_2O_3)

Samples	Frit	Ceramic fillers	
		ZnO	Al_2O_3
BF1	85	10	5
BF2	80	15	5
BF3	75	20	5
BF4	80	10	10
BF5	75	15	10
BF6	70	20	10

using the Archimedes method. The surface morphology of the composites was observed as a function of the reactivity of the glass and filler using field emission scanning electron microscopy (FE-SEM, S-4200, Hitachi, Japan), Energy Dispersive Spectroscopy (EDS), and X-ray diffraction (XRD, DMAX-2500, Rigaku, Japan). The hardness and fracture toughness of the composites were measured using a micro-Vickers hardness tester (HMV-2, Shimadzu, Japan) and FE-SEM. The elastic modulus was determined by a resonance method using an ultrasonic pulser-receiver (Panametrics 5800PR, Panametrics, Japan) and an oscilloscope (TDS 220, Tektronix, UK). The change in the roughness of the composites caused by HNO_3 etching was measured with a surface profiler (Dektak 6M, Veeco, USA). Finally, the surface morphology of the composites etched by 0.5% HNO_3 was observed using FE-SEM.

Results and discussion

From the non-isothermal thermal analysis using DTA with a heating rate of $10\text{ }^\circ\text{C/min}$, the glass transition temperature (T_g) was determined to be $465\text{ }^\circ\text{C}$ for both the bismate glass matrix and glass composites (frits with ZnO and Al_2O_3 fillers). Two onset points of crystallization (T_o) were detected at 548 and $578\text{ }^\circ\text{C}$, respectively, for the BF1 composite. The isothermal thermal analysis was also

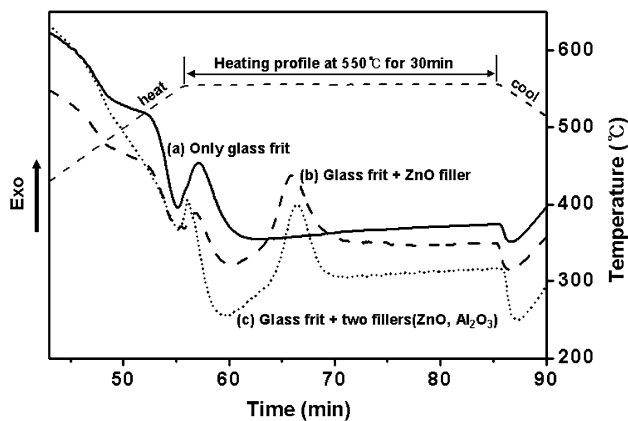


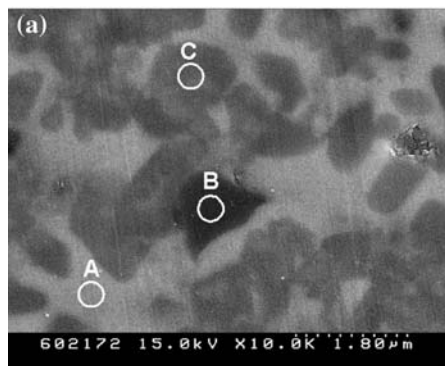
Fig. 2 The isothermal DTA curves of (a) glass frit ($d_{50} = 2.5 \mu\text{m}$), (b) glass frit with ZnO filler and (c) glass frit with ZnO and Al_2O_3 fillers (Condition: heating at $550 \text{ }^\circ\text{C}$ for 30 min)

conducted to investigate the reaction between the glass matrix and ceramics fillers at the firing temperature ($550 \text{ }^\circ\text{C}$), as shown in Fig. 2.

The temperature was increased at a rate of $10 \text{ }^\circ\text{C}/\text{min}$ from room temperature to $550 \text{ }^\circ\text{C}$, which is the firing temperature, held at this temperature for 30 min and then slowly cooled down to room temperature. In the case of the glass frits containing fillers in Fig. 2b and c, two exothermic peaks occurred during firing at $550 \text{ }^\circ\text{C}$ for 30 min. Based on this result, the first exothermic peak might only correspond to the devitrification of the matrix glass and the second one should be done by the formation of a crystal phase related to the reaction between the ZnO filler and the residual glass. The glass frits containing Al_2O_3 filler do not show any crystallization peak, indicating that there was no reaction between the Al_2O_3 filler and bismate glass matrix. In the case of the glass frits containing only ZnO filler, the DTA curve shows an exothermal peak corresponding to the reaction between the filler and glass frits after the temperature reached $550 \text{ }^\circ\text{C}$.

The surface morphology of the composite (BF1) sintered at $550 \text{ }^\circ\text{C}$ was observed by FE-SEM (Fig. 3a), and three regions were quantitatively analyzed by EDS. The

Fig. 3 (a) SEM image and (b) EDS result of composite (BF1) sintered at $550 \text{ }^\circ\text{C}$ for 30 min showing chemical elements in A, B, and C areas from (a)



brighter area (A area in Fig. 3a) was relatively rich in Bi. This region is regarded as the residual glass matrix and the devitrification of the matrix glass. The darker area (B area in Fig. 3a) was rich in aluminum and oxygen, implying that this region is the Al_2O_3 filler. The gray area (C area in Fig. 3a) is regarded as a crystal phase formed by the reaction between the glass matrix and the ZnO filler.

To identify the crystal phases shown in Fig. 3a, XRD analysis was conducted. The XRD pattern of the glass matrix corresponds to a typical amorphous phase (Fig. 4a) and that of the composite containing the ZnO and Al_2O_3 fillers (BF1) shows two crystal phases at room temperature, which are ZnO and Al_2O_3 crystal phases (Fig. 4c). The glass matrix fired at $550 \text{ }^\circ\text{C}$ for 30 min was crystallized into two crystal phases ($\text{Zn}_4\text{O}(\text{BO}_2)_6$ and B_2O_3) as shown in Fig. 4b. Based on our XRD result, B_2O_3 the crystal phase is supposed to be formed from the residual glass matrix, owing to the formation of $\text{Zn}_4\text{O}(\text{BO}_2)_6$ crystal phase. Considering the XRD patterns of the two fillers added to the sintered body, $\text{Zn}_4\text{O}(\text{BO}_2)_6$ crystal phase was again formed due to the reaction between the glass

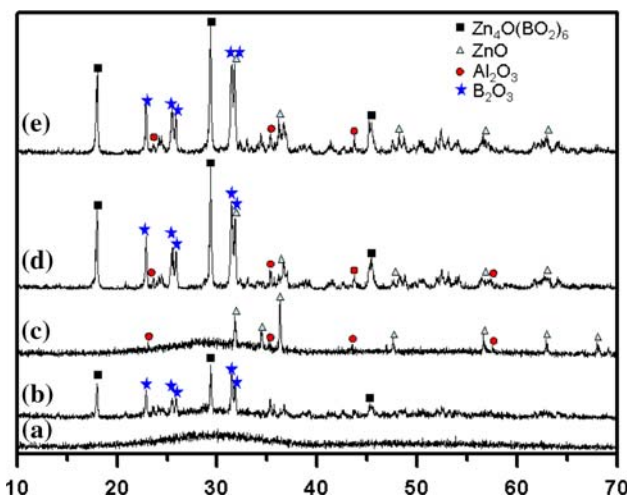
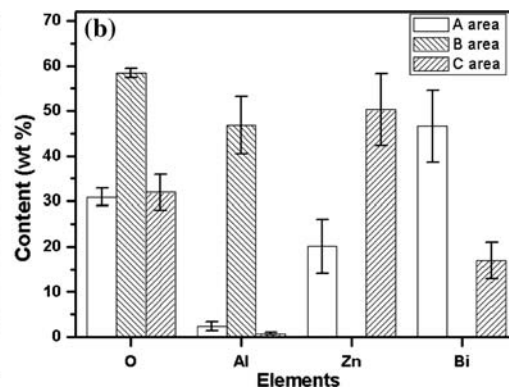


Fig. 4 XRD results of (a) raw material (glass) (b) fired at $550 \text{ }^\circ\text{C}$ (c) raw material (BF1) (d) BF1 fired at $550 \text{ }^\circ\text{C}$ and (e) $590 \text{ }^\circ\text{C}$ for 30 min



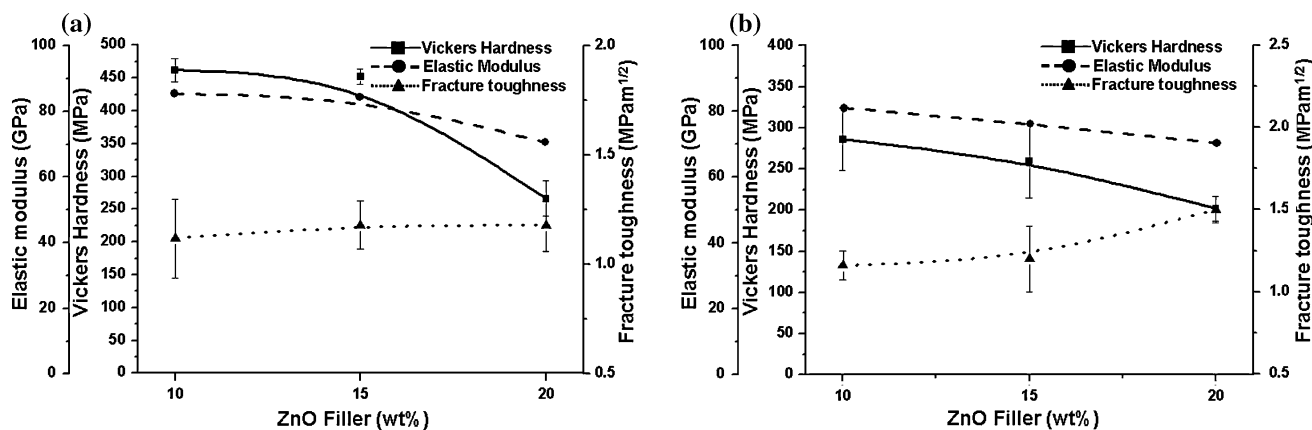


Fig. 5 Distribution of Vickers hardness, elastic modulus, and fracture toughness of (a) 5 wt.% Al₂O₃ and (b) 10 wt.% Al₂O₃ filler-added composites with different ZnO filler contents

matrix and ZnO filler that implies the peak intensity of Zn₄O(BO₂)₆ crystal phase (Fig. 4d). It is considered that after the crystallization in the glass matrix, the glass matrix reacted with the fine ZnO particles, due to the viscous behavior of the residual glass, and then crystallization again occurred around ZnO. When the sintering temperature increases, the viscosity of glass matrix becomes lower. Eventually, it is assumed that the reactivity leading to the formation of Zn₄O(BO₂)₆ was heightened, due to the migration of the ZnO fillers at the high sintering temperature (Fig. 4e). The XRD results also show that there was no reaction related to the Al₂O₃ fillers.

The mechanical properties such as the Vickers hardness, elastic modulus, and fracture toughness are shown in Fig. 5. One effective way to improve the mechanical properties of glass or glass-ceramic is to form a composite material. In this study, the Vickers hardness and elastic modulus of the glass matrix were 435 MPa and 80.7 GPa,

respectively. The mechanical properties of the composites, BF1 and BF2, were slightly improved by the addition of ceramic fillers as a function of reinforcement compared to those of the glass matrix itself, due to the crystalline ceramic filler phase. However, the Vickers hardness and elastic modulus of the composites decreased with increasing content of ZnO and Al₂O₃ fillers, because of the formation of pores and cracks caused by the difference of the coefficient of thermal expansion and density between the glass matrix and new crystal phases.

Considering the fracture toughness, it generally increased with increasing content of the fillers (ZnO, Al₂O₃) and the fracture toughness of the composite, BF6, was the highest among these composites, due to the addition of a relatively large amount of Al₂O₃ filler and the high porosity on the surface (Fig. 5). It is considered that the pores and Al₂O₃ fillers can play a role to increase the crack length, due to the deflection of the cracks, and

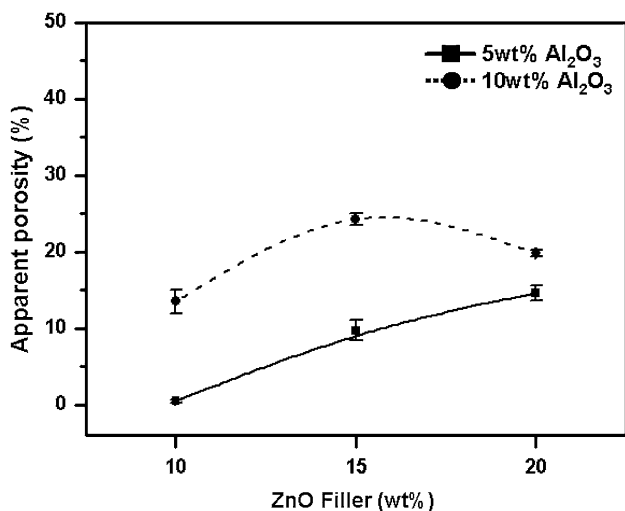


Fig. 6 Distribution of apparent porosity with different filler contents

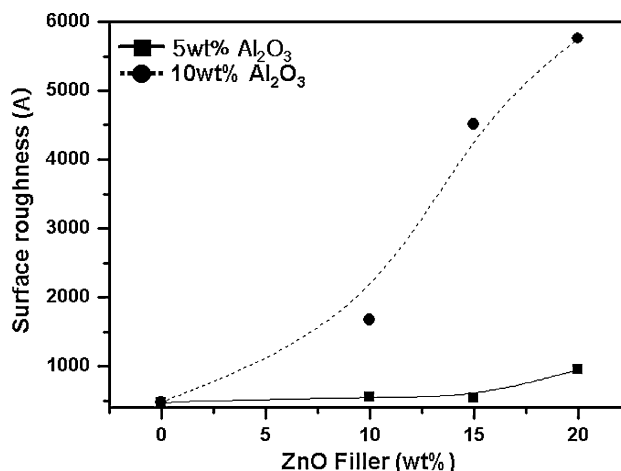
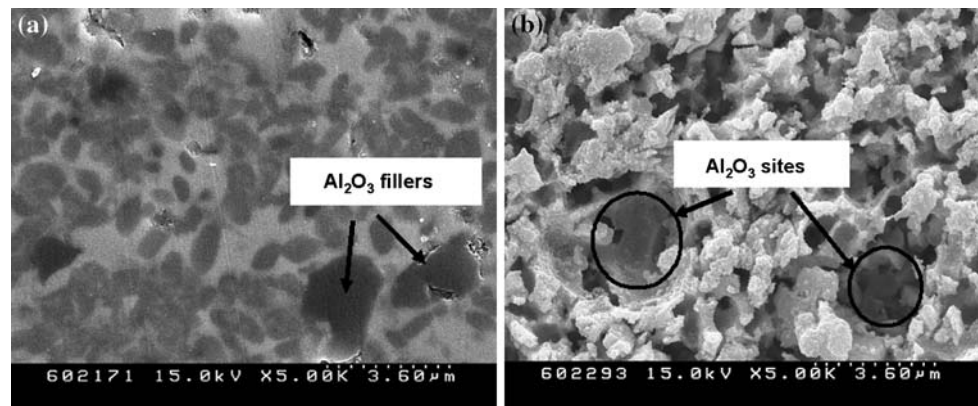


Fig. 7 Roughness changes of as-received and etched composites with different filler contents

Fig. 8 SEM images of glass composite (BF1) (a) before etching and (b) after etching by 0.5% HNO₃ at 45 °C for 10 min



prevent the growth of cracks formed by external force. Furthermore, the movement of the cracks can be interrupted by the creation of new crystal phases, implying the improvement of the fracture toughness [13–15].

In Fig. 6, the porosity of both 5 and 10 wt.% Al₂O₃-added composites increased with increasing content of ZnO filler, because of the resulting increase in the degree of crystallization. Moreover, the porosity of the 10 wt.% Al₂O₃-added composites was higher than that of the 5 wt.% Al₂O₃-added composites. There was no reaction between the glass matrix and the Al₂O₃ filler according to the DTA and XRD results (Figs. 2 and 4). Therefore, the particle rearrangement process of the Al₂O₃ fillers takes place during firing. At this time, many open pores were formed around the Al₂O₃ fillers due to the difference in density between the glass matrix and Al₂O₃ filler, implying an increase of the porosity [16].

The porosity would be expected to affect the etching efficiency during the etching process for barrier-ribs, as well as the mechanical properties. To determine the effect of the porosity on the etching efficiency, the change in roughness between the as-received composites and those etched by 0.5% HNO₃ was measured using a surface profiler (Fig. 7). The changes in roughness of the 5 wt.% Al₂O₃-added composites increased gradually with increasing content of ZnO filler, but the overall change was very small. In the case of the 10 wt.% Al₂O₃-added composites, the change in roughness increased sharply with increasing content of ZnO filler. Namely, the etching efficiency of the composites was improved by increasing the porosity and content of the ZnO filler. Among the various crystal phases present in the composite, a specific crystal phase, which is the Zn₄O(BO₂)₆ crystal phase in this study, is dissolved before anything else. Then, other crystal phases and the Al₂O₃ filler are etched as a cluster.

The surface morphology of the glass composite (BF1) etched by 0.5% HNO₃ at 45 °C is shown in Fig. 8. It shows a very rough surface due to the optional etching by the acid (HNO₃). The numerous holes on the surface in Fig. 8b are

regarded as the sites of Al₂O₃ fillers after etching. We consider that this rough surface is suitable to bond physically on barrier-ribs when spreading phosphors. The etching process for barrier-ribs in the PDP industry is completed within a short time (several tenths of a second), implying the importance of the etching efficiency.

Conclusion

The mechanical and etching properties of composites, ZnO and Al₂O₃ fillers added in Bi₂O₃–ZnO–B₂O₃–Al₂O₃ glass matrix with different contents, were investigated. When the content of the fillers was increased, the Vickers hardness and elastic modulus decreased and the fracture toughness and etching efficiency increased, due to the effect of the porosity and newly formed crystal phases. The porosity and degree of crystallization of the composites could be controlled by adjusting the content of the ZnO and Al₂O₃ fillers. In this study, we understood the roles of the ceramic fillers (ZnO, Al₂O₃) used for the barrier-ribs in PDPs, implying the effect of quantitatively and qualitatively suitable filler addition on the mechanical properties and etching properties.

Acknowledgement This work was partially supported by the Ministry of Education and Human Resources Development (MOE), the Ministry of Commerce, Industry and Energy (MOCIE), and the Ministry of Labor (MOLAB) through the fostering project of the Lab of Excellency and was supported by the Ministry of Commerce, Industry and Energy (MOCIE) through the New Growth Engine Project.

References

1. Oversluizen G, De Zwart S, Gillies MF, Dekker T, Vink TJ (2004) *Microelectron J* 35:319
2. Kim YD, Park SK (2006) *Displays* 27:62
3. Cho IH, Jeong SC, Park JM, Jeong HD (2001) *J Mater Process Technol* 13:355

4. Nitta A, Koide M, Matusita K (2001) *Phys Chem Glasses* 42:275
5. Kim DN, Lee JY, Huh JS, Kim HS (2002) *J Non-Cryst Solids* 306:70
6. Park JH, Kim HS (2003) *J Mat Sci Lett* 22:1197
7. Morena R (2000) *J Non-Cryst Solids* 263–264:382
8. Kim SG, Park JS, An JS, Hong KS, Shin HH, Kim HS (2006) *J Am Ceram Soc* 89:902
9. Kim YJ, Hwang SJ, Kim HS (2006) *Mater Sci Forum* 510–511:578
10. Kim SG, Shin H, Park JS, Hong KS, Kim H (2005) *J Electroceram* 15:129
11. Shin H, Kim SG, Park JS, An JS, Hong KS, Kim H (2006) *J Am Ceram Soc* 89:3258
12. Shin H, Park JS, Kim SG, Jung HS, Hong KS, Kim H (2006) *J Mater Res* 21:1753
13. Kavouras P, Charitidis C, Karakostas Th (2006) *J Non-Cryst Solids* 352:5515
14. Todd RI, Boccaccini AR, Sinclair R, Yaltee RB, Young RJ (1999) *Acta Mater* 47:3233
15. El-Kheshen AA, Znwrah MF (2003) *Ceram Int* 29:251
16. Bernardo E, Scarinci G, Hreglich S (2006) *J Eur Ceram Soc* 25:1541